Arabian Journal of Chemistry (2015) xxx, xxx–xxx

King Saud University

Arabian Journal of Chemistry

www.ksu.edu.sa
www.sciencedirect.com

ORIGINAL ARTICLE

Potentiometric and antimicrobial studies on the asymmetric Schiff bases and their binuclear Ni(II) and Fe(III) complexes; synthesis and characterization of the complexes

Özlem Güngör [1], **Perihan Gürkan** *

Department of Chemistry, Faculty of Science, Gazi University, Teknikokullar, Ankara 06500, Turkey

Received 5 March 2013; accepted 12 February 2015

KEYWORDS

Schiff bases;
Asymmetric diimines;
Nickel(II) complexes;
Iron(III) complexes;
Potentiometry;
Antimicrobial activity

Abstract The protonation constants of two nitro-Schiff bases **SB**[1], **SB**[2] and three asymmetric tetradentate diimines $\mathbf{H_2L^1}$, $\mathbf{H_2L^2}$ and $\mathbf{H_2L^3}$ and the stability constants of their ML type binuclear Ni(II) and Fe(III) complexes have been determined potentiometrically. The asymmetric diimines are (2OH) R—CH=N—C_6H_4—CH=N—R′ (2OH) type compounds [where R = R′ = phenyl for $\mathbf{H_2L^1}$; R = naphthyl, R′ = phenyl for $\mathbf{H_2L^2}$ and R = R′ = naphthyl for $\mathbf{H_2L^3}$]. The effect of tautomeric forms on the acid-base properties of the diimines has been investigated and discussed. In addition, dimeric and binuclear Ni(II) and Fe(III) complexes of the diimines have been synthesized and characterized by physical and spectroscopic techniques. Also, *in vitro* antimicrobial activities of the diimines and the complexes have been evaluated against three bacteria: *Micrococcus luteus* (NRLL B-4375), *Bacillus cereus* (RSKK 863), *Escherichia coli* (ATCC 11230) and the fungus: *Candida albicans* (ATCC 10239).

1. Introduction

Symmetrical diimine Schiff bases (—CH=N—Ar—N=CH—) or (—N=HC—Ar—CH=N—) type can be obtained easily from aromatic diamines with two mol of an aldehyde or aromatic dialdehydes with two mol of an amine, respectively (Sözen et al., 2007; Kumari et al., 2008; Hou et al., 2007). But, asymmetrical diimine Schiff bases (—CH=N—Ar—CH=N—) type cannot be synthesized directly. In our previous works (Güngör and Gürkan, 2010; Nartop et al., 2008; Güngör, 2008; Sürücüoğlu, 2008), we reported a new synthetic method for asymmetric diimines named above. Although, large

* Corresponding author. Tel.: +90 312 202 11 18; fax: +90 312 212 22 79.
E-mail addresses: ozlemgungor@gazi.edu.tr (Ö. Güngör), pgurkan@gazi.edu.tr (P. Gürkan).
[1] Tel.: +90 312 202 11 47; fax: +90 312 212 22 79.

Peer review under responsibility of King Saud University.

Production and hosting by Elsevier

http://dx.doi.org/10.1016/j.arabjc.2015.02.009
1878-5352

Please cite this article in press as: Güngör, Ö., Gürkan, P. Potentiometric and antimicrobial studies on the asymmetric Schiff bases and their binuclear Ni(II) and Fe(III) complexes; synthesis and characterization of the complexes. Arabian Journal of Chemistry (2015), http://dx.doi.org/10.1016/j.arabjc.2015.02.009

numbers of publications are available on determination of the protonation constants of symmetrical diimines and their metal complexes (Galic et al., 1997; Mashhadizadeh et al., 2003; Shokrollahi et al., 2011; Hernández-Molina et al., 1997), the protonation constants of asymmetrical diimines have not been determined yet.

In this paper, we have reported the protonation constants of three new asymmetric diimines (**H_2L^1, H_2L^2 and H_2L^3**) and the stability constants of their ML-type Ni(II) and Fe(III) complexes in 1: 1 (v: v) ethanol–water mixture at 25.0 ± 0.1 °C and 0.50 M KCl ionic strength. Two nitro-Schiff bases (**SB^1, SB^2**) have been also studied potentiometrically. Numerical values of the protonation constants were discussed in terms of tautomeric forms.

In the present work, we have synthesized and characterized the solid Ni(II) and Fe(III) complexes of the asymmetric diimine ligands. Additionally, *in vitro* antimicrobial activities of the diimines and their complexes have been tested against three bacteria: *Micrococcus luteus* (NRLL B-4375), *Bacillus cereus* (RSKK 863), *Escherichia coli* (ATCC 11230) and the fungus: *Candida albicans* (ATCC 10239). It was shown that, all of the diimines and **NiL^1, FeL^1** and **FeL^2** complexes have an antimicrobial effect on all the studied microorganisms; **NiL^2** and **FeL^3** complexes seem to be inactive against *B. cereus* and **NiL^3** complex is inactive against *B. cereus* and *E. coli*.

2. Experimental

2.1. Materials and reagents

Nickel(II) and iron(III) chlorides were obtained from Aldrich Chemical Company and used without further purification. The solvents used were of spectroscopic grade.

2.2. Synthesis

2.2.1. Synthesis of the nitro-Schiff bases and the asymmetric diimines

The nitro-Schiff bases (**SB^1** and **SB^2**) and the asymmetric diimines (**H_2L^1**, **H_2L^2** and **H_2L^3**) were synthesized as described in our previous work (Güngör and Gürkan, 2010).

2.2.2. Synthesis of the complexes: general procedure

The asymmetric diimine ligand (1 mmol) was dissolved in absolute ethanol (50 mL). The ethanolic solution of Ni(II) or Fe(III) chlorides (1 mmol, 10 mL) was added dropwise to the solution of ligand. The reaction mixture was refluxed for 6 h for L^1Ni and L^1Fe; 4 h for the others at 70 °C. The mixture was kept over a period of 2 days for L^3Ni and L^3Fe; 3 days for L^2Ni and L^2Fe and 5 days for L^1Ni and L^1Fe. The solid product was filtered, washed with 40 mL of hot water, ethanol and diethyl ether respectively, and then dried in a vacuum desiccator over anhydrous $CaCl_2$.

2.2.2.1. Complex ***NiL^1***. Green solid; Yield 46%, m.p > 360 °C. Anal. for $[Ni(C_{20}H_{14}N_2O_2)(H_2O)_2]_2$ (816) Calc. C58.82, H4.41, N6.86, Ni14.39. Found C58.89, H4.60, N6.39, Ni13.63. IR (KBr, cm^{-1}); ν (H_2O) 3436(w), ν (Ar—H) 3057(w), ν (C═C) 1621(s), ν (CH═N) 1607(s) and 1565(w), ν (C—O) 1126(m), ν (M—O) 502(w), ν (M—N) 446(m). MS: $(M)^+$ (*m*/*z*): 816 (0.3%), 810 (4.4%), 726 (29.0%), 580 (2.4%), 480 (2.3%), 314 (40.8%), 286 (43.4%), 214 (100%), 110 (23.8%). Paramagnetic (μ = 2.59 BM) and nonelectrolytic complex (Λ = 1.90 Ω^{-1} cm^2 mol^{-1}; in 10^{-3} M DMSO).

2.2.2.2. Complex ***FeL^1***. Black solid; Yield 51%, m.p > 360 °C. Anal. for $[Fe(C_{20}H_{14}N_2O_2)(H_2O)Cl]_2{\cdot}H_2O$ (864) Calc. C55.56, H3.94, N6.48, Fe12.93. Found C54.92, H3.56, N6.12, Fe11.77. IR (KBr, cm^{-1}); ν (H_2O) 3436(m), ν (Ar—H) 3070(m), ν (C═C) 1602(s), ν (CH═N) 1579(m) and 1574(s), ν (C—O) 1129(w), ν (M—O) 457(w), ν (M—N) 434(w). MS: $(M+6)^+$ (*m*/*z*): 870 (5.7%), 864 (0.1%), 746 (12.9%), 579 (4.5%), 551 (42.9%), 480 (5.5%), 312 (0.2%), 267 (100%), 202 (1.3%). Paramagnetic (μ = 4.90 BM) and nonelectrolytic complex (Λ = 19.70 Ω^{-1} cm^2 mol^{-1}; in 10^{-3} M DMF).

2.2.2.3. Complex ***NiL^2***. Green solid; Yield 60%, m.p > 360 °C. Anal. for $[Ni(C_{24}H_{16}N_2O_2)]_2$ (844) Calc. C68.25, H3.79, N6.64, Ni13.91. Found C67.69, H3.75, N5.97, Ni12.86. IR (KBr, cm^{-1}); ν (Ar—H) 3044(w), ν (C═C) 1613(m), ν (CH═N) 1598(m) and 1573(m), ν (C—O) 1280(m), ν (M—O) 527(w), ν (M—N) 473(w). MS: (*m*/*z*): 583 (0.8%), 356 (2.1%), 330 (1.9%), 282 (2.1%), 264 (100%), 144 (1.7%), 90 (1.0). Diamagnetic (μ = 0 BM) and nonelectrolytic complex (Λ = 0.63 Ω^{-1} cm^2 mol^{-1}; in 10^{-3} M DMSO).

2.2.2.4. Complex ***FeL^2***. Black solid; Yield 54%, m.p > 360 °C. Anal. for $[Fe(C_{24}H_{16}N_2O_2)(H_2O)Cl]_2$ (946) Calc. C60.89, H3.81, N5.92, Fe11.81. Found C59.95, H3.10, N5.65, Fe12.07. IR (KBr, cm^{-1}); ν (H_2O) 3300(m), ν (Ar—H) 3063(m), ν (C═C) 1613(s), ν (CH═N) 1596(s) and 1570(s), ν (C—O) 1300(m), ν (M—O) 560(m), ν (M—N) 457(w). MS: $(M+4)^+$ (*m*/*z*): 950 (1.6%), 896 (2.5%), 747 (4.1%), 669 (3.5%), 598 (2.9%), 395 (100%), 356 (1.8%), 317 (89.3%), 282 (4.6%), 264 (1.7%), 153 (2.5%), 79 (28.2%). Paramagnetic (μ = 5.25 BM) and nonelectrolytic complex (Λ = 41.96 Ω^{-1} cm^2 mol^{-1}; in 10^{-3} M DMSO).

2.2.2.5. Complex ***NiL^3***. Brown solid; Yield 58%, m.p > 360 °C. Anal. for $[Ni(C_{28}H_{18}N_2O_2)]_2$ (944) Calc. C71.19, H3.81, N5.93, Ni12.44. Found C70.80, H3.76, N5.52, Ni12.66. IR (KBr, cm^{-1}); ν (Ar—H) 3051(w), ν (C═C) 1626(m), ν (CH═N) 1599(m) and 1529(m), ν (C—O) 1271(m), ν (M—O) 521(w), ν (M—N) 476(m). MS: $(M+1)^+$ (*m*/*z*): 945 (0.2%), 730 (2.0%), 417 (3.9%), 314 (100%), 230 (58.1%), 170 (10.6%), 115 (1.8%), 79 (81.5%). Diamagnetic (μ = 0 BM) and nonelectrolytic complex (Λ = 2.60 Ω^{-1} cm^2 mol^{-1}; in 10^{-3} M DMSO).

2.2.2.6. Complex ***FeL^3***. Black solid; Yield 63%, m.p > 360 °C. Anal. for $[Fe(C_{28}H_{18}N_2O_2)(H_2O)Cl]_2$ (1046) Calc. C64.24, H3.82, N5.35, Fe10.68. Found C64.30, H4.00, N5.20, Fe9.04. IR (KBr, cm^{-1}); ν (H_2O) 3423(m), ν (Ar—H) 3056(m), ν (C═C) 1626(s), ν (CH═N) 1606(s) and 1542(s), ν (C—O) 1300(m), ν (M—O) 573(w), ν (M—N) 470(m). MS: $(M)^+$ (*m*/*z*): 1046 (2.9%), 779 (2.4%), 645 (2.1%), 445 (100%), 418 (0.5%), 314 (24.2%), 286(21.7%), 230 (6.4%), 160(0.8), 115 (0.9%), 79(28.7%). Paramagnetic (μ = 5.25 BM) and nonelectrolytic complex (Λ = 12.80 Ω^{-1} cm^2 mol^{-1}; in 10^{-3} M DMSO).

Please cite this article in press as: Güngör, Ö., Gürkan, P. Potentiometric and antimicrobial studies on the asymmetric Schiff bases and their binuclear Ni(II) and Fe(III) complexes; synthesis and characterization of the complexes. Arabian Journal of Chemistry (2015), http://dx.doi.org/10.1016/j.arabjc.2015.02.009

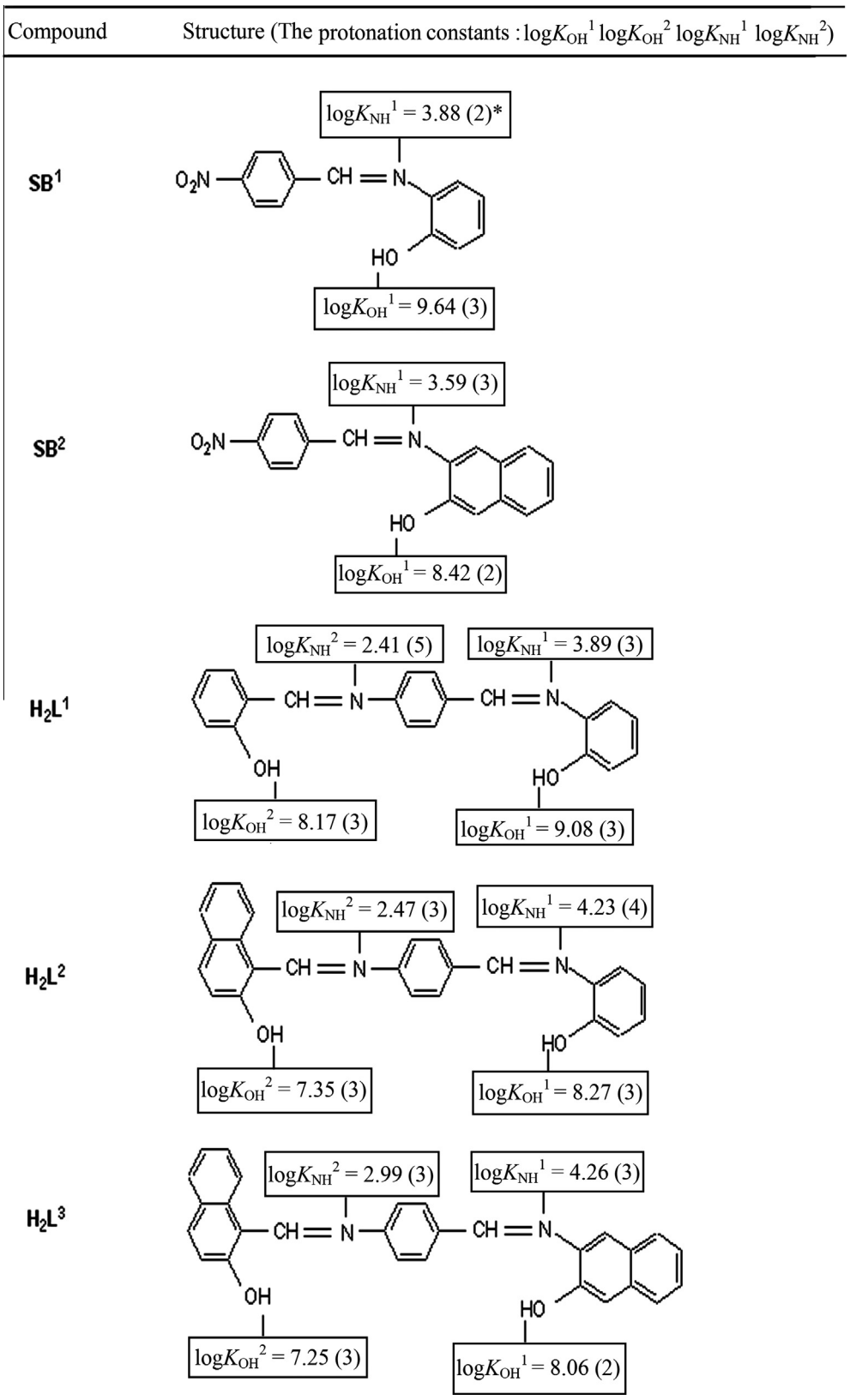

Figure 1 The structures and the protonation constants of all the Schiff bases in 1:1 (v:v) ethanol–water solution at 25.0 ± 0.1 °C (*values in parentheses are standard deviations, and they are less than 0.01 for all of the constants).

Please cite this article in press as: Güngör, Ö., Gürkan, P. Potentiometric and antimicrobial studies on the asymmetric Schiff bases and their binuclear Ni(II) and Fe(III) complexes; synthesis and characterization of the complexes. Arabian Journal of Chemistry (2015), http://dx.doi.org/10.1016/j.arabjc.2015.02.009

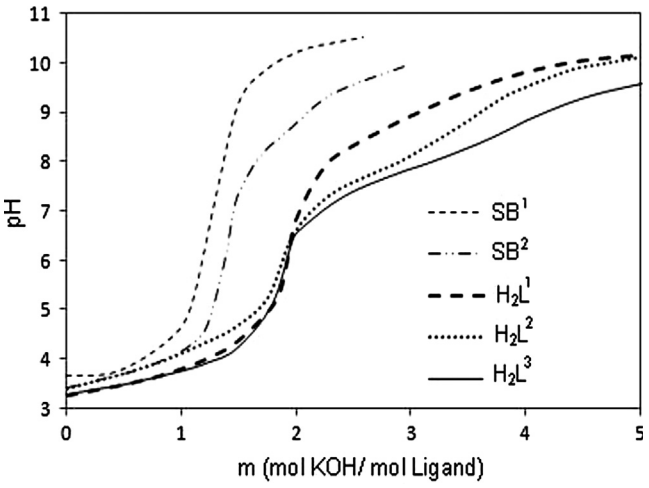

Figure 2 Potentiometric titration curves for the nitro-Schiff bases and the diimines.

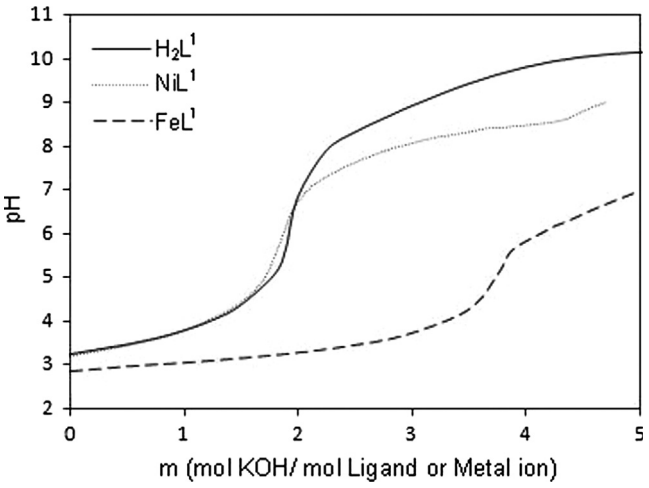

Figure 4 Potentiometric titration curves of nickel(II) and iron(III) complexes of $\mathbf{H_2L^1}$.

2.3. Instrumentation

Infrared absorption spectra in the 4000–400 cm^{-1} range were recorded using KBr discs on a Mattson 1000 FTIR spectrophotometer. Carbon, hydrogen and nitrogen analyses were obtained using GmbH vario MICRO CHNS analyzer. The mass spectra (LC–MS/ESI) were recorded at 70 eV on an Agilent 1100 MSD spectrometer. Melting points were measured on a Gallenkamp apparatus using a capillary tube. The TGA curves of complexes were recorded using a Du Pont Instrument 951 between 35 and 800 °C at heating rate of 10 °C min^{-1} in a N_2 atmosphere. The room temperature magnetic susceptibilities were determined using a Sherwood Scientific MKI model Evans magnetic balance. Conductivity measurements were carried out at 25 °C in 10^{-3} M dimethyl sulfoxide (DMSO) or 10^{-3} M N,N-dimethyl formamide (DMF) using a Siemens WPA CM 35 apparatus. Metal ion solutions were standardized by VARIAN AA 240FS model Fast Sequential Atomic Absorption Spectrometer. Ultraviolet–visible spectra of the complexes in DMSO were recorded using Analytik Jena UV-200 spectrophotometer, over the wavelength range 400–900 nm at room temperature. MIC values of diimine $\mathbf{H_2L^1}$ were determined in Gazi University–Molecular Biology Research and Training Center (MOBAM). XRD was recorded on a APD 2000 PRO X-ray diffractometer with Cu Kα radiation (λ = 1.54059 Å) in the 2θ = 0–70° range.

2.4. Potentiometric reagents and solutions

The potentiometric measurements in this study were carried out in 1: 1 (v: v) aqueous-ethanol media. Ethanol was purchased from Merck and used without further purification. Doubly distilled and CO_2 free water was used exclusively.

Stock solutions of strong acid and strong base were prepared using analytical reagent grade 0.10 M HCl solution (Merck) and 0.10 M KOH solution (Merck), respectively. The 0.0051 M KOH solution was standardized by titration against the primary standard oxalic acid dihydrate (Aldrich). The 0.0506 M HCl solution was prepared and then standardized by titration with 0.0051 M KOH solution. During each titration the ionic strength was maintained at 0.50 M KCl (Merck, extra pure).

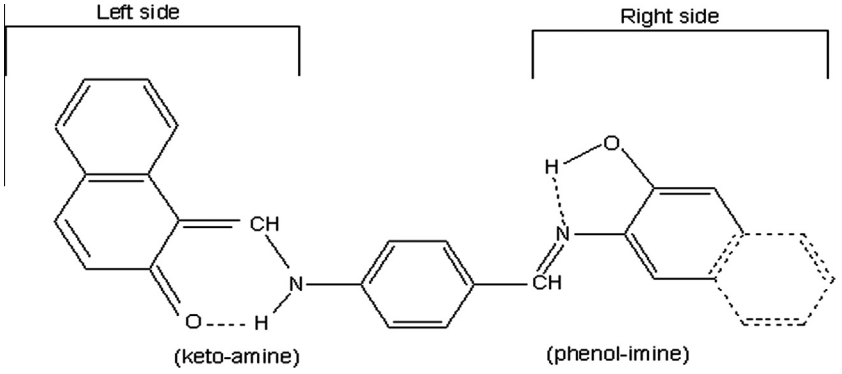

Figure 3 Tautomeric forms of the H_2L^2 and $\mathbf{H_2L^3}$.

Please cite this article in press as: Güngör, Ö., Gürkan, P. Potentiometric and antimicrobial studies on the asymmetric Schiff bases and their binuclear Ni(II) and Fe(III) complexes; synthesis and characterization of the complexes. Arabian Journal of Chemistry (2015), http://dx.doi.org/10.1016/j.arabjc.2015.02.009

Table 1 The stability constants of Ni(II) and Fe(III) complexes at 25.0 ± 0.1 °C, for 1:1 (v:v) ethanol–water mixture (μ = 0.50 M KCl).

Compound	Log K_{ML}	Compound	Log K_{ML}	Compound	Log K_{ML}
NiL^1	9.43 ± 0.03	**NiL^2**	7.20 ± 0.08	**NiL^3**	12.55 ± 0.08
FeL^1	8.21 ± 0.10	**FeL^2**	9.56 ± 0.06	**FeL^3**	11.85 ± 0.08

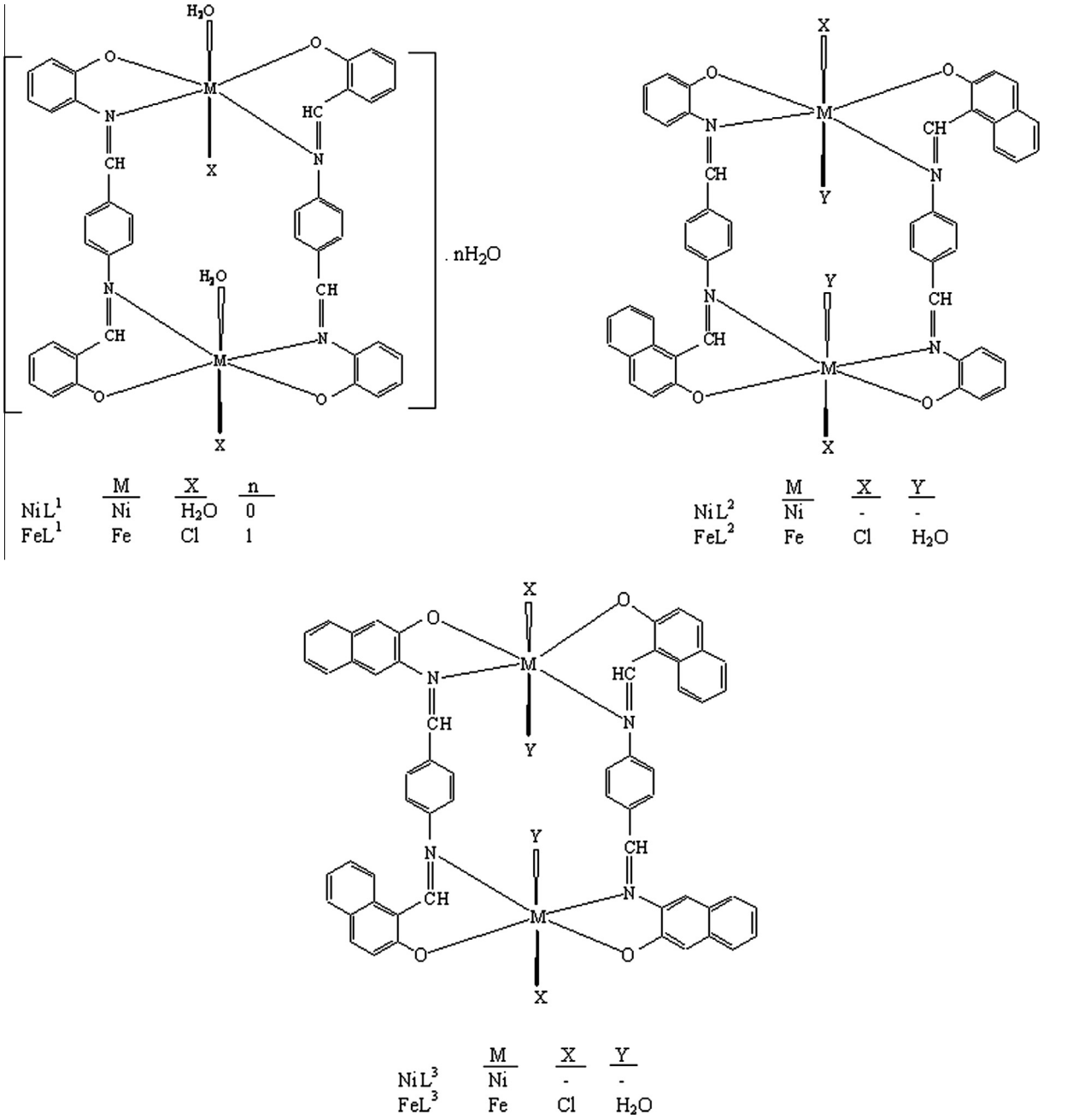

Figure 5 The suggested structures of the complexes.

Please cite this article in press as: Güngör, Ö., Gürkan, P. Potentiometric and antimicrobial studies on the asymmetric Schiff bases and their binuclear Ni(II) and Fe(III) complexes; synthesis and characterization of the complexes. Arabian Journal of Chemistry (2015), http://dx.doi.org/10.1016/j.arabjc.2015.02.009

All metal ion solutions were prepared from their analytical grade chlorides and standardized by atomic absorption spectroscopy method.

2.5. Potentiometric measurements

All potentiometric measurements were performed in a double walled glass cell that was thermostated at 25.0 ± 0.1 °C. Electrode system was kept in 1:1 (v:v) aqueous-ethanol media. A Jenway pH-meter equipped with an ISE combined glass electrode was used for titrations.

The system was calibrated to read the hydrogen ion concentration by titration of HCl solution with KOH solution in 0.50 M KCl ionic strength according to Gran's method (Gran, 1952; Sarı et al., 2003). Small amounts of titrant (0.05 mL) KOH solution were added with a microburette. Solutions were titrated between the pH range 3–10 for the ligands, 3–9 for the nickel(II) complexes, but 3–6 for the iron(III) complexes to avoid the precipitations. Concentrations of the nitro-Schiff bases and the asymmetric diimines were between 3.9×10^{-4} and 4.6×10^{-4} M and metal-to-ligand ratios were 1:4 for Ni(II) and 1:8 for Fe(III). pH corrections for aqueous-organic system were done as described in the literature (van Uitert and Haas, 1953; Belaid et al., 2007).

The following solutions (total volume = 25.0 ± 0.01 mL) were titrated potentiometrically with 0.0051 M KOH solution:

(i) HCl + KCl.
(ii) HCl + KCl + ligand.
(iii) HCl + KCl + ligand + metal ion.

The computations of the protonation constants of the nitro-Schiff bases and the asymmetric diimines from potentiometric data were carried out with the PKAS computer program (Martell and Motekaitis, 1988). The experimental method of Bjerrum and Calvin as modified by Irving and Rossotti (1954) was used to determine $\check{n}$, $\check{n}_A$ and pL values. The stability constants of the complexes were calculated using the equation

$$\log K = pL + \log(\check{n}/1-\check{n}) \quad (A.1)$$

2.6. Antimicrobial screening

In vitro antimicrobial activities of the asymmetric diimines (**H_2L^1**, **H_2L^2** and **H_2L^3**) and their Ni(II) and Fe(III) complexes were tested using the well-diffusion method (Nartop et al., 2008) against the bacteria: *M. luteus* (NRLL B-4375), *B. cereus* (RSKK 863), *E. coli* (ATCC 11230) in Molten Nutrient Agar medium and the fungus: *C. albicans* (ATCC 10239) in YPD Agar medium.

The bacterial strains were inoculated into Molten Nutrient Broth and incubated at 37 °C for 18 h. The yeast cells were inoculated into YPD Broth and incubated at 37 °C for 18 h. The test solutions of 10 mg mL^{-1} and 4 mg mL^{-1} in DMSO were prepared for all the diimines and the complexes, respectively. The YPD Agar (15 mL) kept at ca. 45 °C, was then poured in the petri-dishes which were inoculated with strains of yeast by taking 100 μL from cell culture media, and allowed to solidify. Then holes of 6 mm diameter were punched carefully using a sterile cork borer and these holes were filled with 50 μL of the test solutions. Petri-dishes were incubated for 24 h for bacteria and 48 h for fungi at 37 °C. The mean value obtained for the three holes was used to calculate the zone of growth inhibition of each sample. DMSO alone was used as a control under the same condition for each microorganism. MIC values (μg mL^{-1}) of **H_2L^1** were done using serial dilutions (1, 2, 4, 8, 16, 32, 63, 125, 250, 500, 1000 μg/mL).

3. Results and discussion

3.1. Ligand protonation constants

Stoichiometric protonation constant values and potentiometric titration curves of the nitro-Schiff bases (**SB^1** and **SB^2**) and the asymmetric diimines (**H_2L^1**, **H_2L^2** and **H_2L^3**) are presented in Figs. 1 and 2 respectively.

The nitro-Schiff bases have two protonation constants: first constant ($\log K^1_{OH}$) refers to the protonation of phenolate anion for **SB^1** and naphtholate anion for **SB^2**, second constant ($\log K^1_{NH}$) belongs to the protonation of imine nitrogen for both. As can be seen in Fig. 2, the breaks near $m = 1$ for the **SB^1** and **SB^2** arise from releasing one hydrogen ion from the protonated form of the ligands. Both of the $\log K^1_{OH}$ and $\log K^1_{NH}$ values of **SB^2** are found lower than that of the **SB^1**. Hence, in the case of **SB^2**, the electron densities of imine nitrogen and naphtholate oxygen atoms are smaller. It may be resulting from the higher electron withdrawing effect of the naphthalene ring compared with the benzene ring. This approach is in line with a literature report for similar compounds (Gündüz et al., 1993; Köseoğlu et al., 1995).

The asymmetric diimines consist of two different fragments bound to central 1,4-phenylene ring:

(1) On the left side, salicyl/naphthaldimine fragment attaches to the center by nitrogen atom. It may form a six membered chelate ring with intramolecular hydrogen bond.
(2) Phenyl/naphthyl azomethine moiety links by carbon atom to the center on the right side. It may also form five membered chelate ring with intramolecular hydrogen bond.

The asymmetric diimines have four protonation constants: first and second constants ($\log K^1_{OH}$ and $\log K^2_{OH}$) correspond to the protonation of phenolate and naphtholate anions, third and fourth constants ($\log K^1_{NH}$ and $\log K^2_{NH}$) refer to protonation of imine nitrogen atoms.

Protonated form of the diimines has four acidic hydrogen atoms and can be shown as $[H_4L]^{2+}$. Two hydrogens are attached to the imine nitrogen atoms and they are neutralized in the pH region 3–5. The breaks near $m = 2$ for their titration curves are due to the appearing of two hydrogen ion from the protonated form of the ligands (in Fig. 2). Other hydrogen ions are bounded to oxygen atoms of the hydroxyl groups and are neutralized between pH 8 and 10. After first two protonations, molecules return to neutral H_2L forms and tautomerism occurs.

The phenol–imine and keto–amine tautomers are formed for the aromatic Schiff bases that have the hydroxyl group in ortho position to the imino group. If the hydrogen atom is completely transferred to the imino nitrogen atom,

Please cite this article in press as: Güngör, Ö., Gürkan, P. Potentiometric and antimicrobial studies on the asymmetric Schiff bases and their binuclear Ni(II) and Fe(III) complexes; synthesis and characterization of the complexes. Arabian Journal of Chemistry (2015), http://dx.doi.org/10.1016/j.arabjc.2015.02.009

keto–amine tautomer is formed (Ünver et al., 2001). In the case of weak hydrogen bond between them, phenol–imine tautomer is protected (Ünver et al., 2006; Hökelek et al., 2000).

In our previous work (Güngör and Gürkan, 2010), we investigated the phenol–imine and keto–amine tautomerism of the diimines ($\mathbf{H_2L^1}$, $\mathbf{H_2L^2}$ and $\mathbf{H_2L^3}$) with spectroscopic methods. We concluded that, in methanol solution, only phenol–imine tautomer was formed on both sides of $\mathbf{H_2L^1}$. On the other hand, for $\mathbf{H_2L^2}$ and $\mathbf{H_2L^3}$, ketoamine tautomer was dominant (about 60%) on the left side, while phenol–imine tautomer was formed on the right side, as shown in Fig. 3.

The effect of the tautomeric forms on the protonation constants can be interpreted as follows:

(i) for $\mathbf{H_2L^1}$, the phenol–imine tautomer only occurs on both left and right side of the molecule. The $\log K^1_{OH}$ and $\log K^2_{OH}$ values (9.08 and 8.17) are related with the protonation of the phenolic oxygen atoms.
(ii) for $\mathbf{H_2L^2}$ and $\mathbf{H_2L^3}$, the phenol–imine tautomer forms on the right side of the molecules (see Fig. 3). The $\log K^1_{OH}$ values (8.27 and 8.06) of these molecules refer to the protonation of the phenolic oxygen atoms. On the other hand, the keto–amine tautomer forms predominantly on the left side of the molecules. Hence, $\log K^2_{OH}$ values (7.35 and 7.25) of these molecules are preferably related with the protonation of less acidic keto oxygen atoms as shown in Fig. 3.
(iii) for all of the diimines, $\log K^2_{NH}$ value of the nitrogen atom on the left side is lower than that of on the right side ($\log K^1_{NH}$) of the molecule. It indicates that the basicity of the nitrogen atom on the left side is less than the other side. It can be explained by the increasing probability of (O—H. . .N) intramolecular hydrogen bonding in six membered chelate ring.

3.2. Complex stability constants

At first, the complex forming reaction was investigated. For this purpose, the titrations of Ni(II) and Fe(III) ions to $\mathbf{H_2L^1}$ ligand in 1: 1 molar ratios were performed. The data are shown in Fig. 4. The break near $m = 4$ for the systems shows the release of four hydrogen ions from the protonated form of the ligand when complexes are formed. Hence, complex forming reactions can be given as follows:

$$[H_4L]^{2+} + M^{n+} \leftrightarrow ML^{(n-2)} + 4H^+$$

The stability constants of the complexes are listed in Table 1. The constants increase in the order $\mathbf{NiL^2} < \mathbf{NiL^1} < \mathbf{NiL^3}$ for Ni(II) complexes while $\mathbf{FeL^1} < \mathbf{FeL^2} < \mathbf{FeL^3}$ for Fe(III) complexes. The stability constant of $\mathbf{H_2L^3}$ ligand with the two metal ions is the biggest. This may be attributed to increasing electron delocalization of two naphthalene rings in the $\mathbf{H_2L^3}$ molecule.

3.3. Structure of the complexes

The proposed molecular formulas of the complexes are given in Fig. 5. After the reaction of ONNO type tetradentate diimines with Ni(II) chloride, dimeric and binuclear $[NiL]_2$ type square planar complexes are formed for $\mathbf{H_2L^2}$ and $\mathbf{H_2L^3}$, while $[NiL(H_2O)_2]_2$ type octahedral complex is formed for $\mathbf{H_2L^1}$. On the other hand, reaction of diimines with Fe(III) chloride gives the octahedral complexes of the type $[FeL(H_2O)Cl]_2{\cdot}nH_2O$ ($n = 0, 1$).

All of the complexes are powder; they are stable at room temperature, insoluble in water and slightly soluble in polar organic solvents. Their melting points are above 360 °C. The molar conductance values of the complexes are measured to

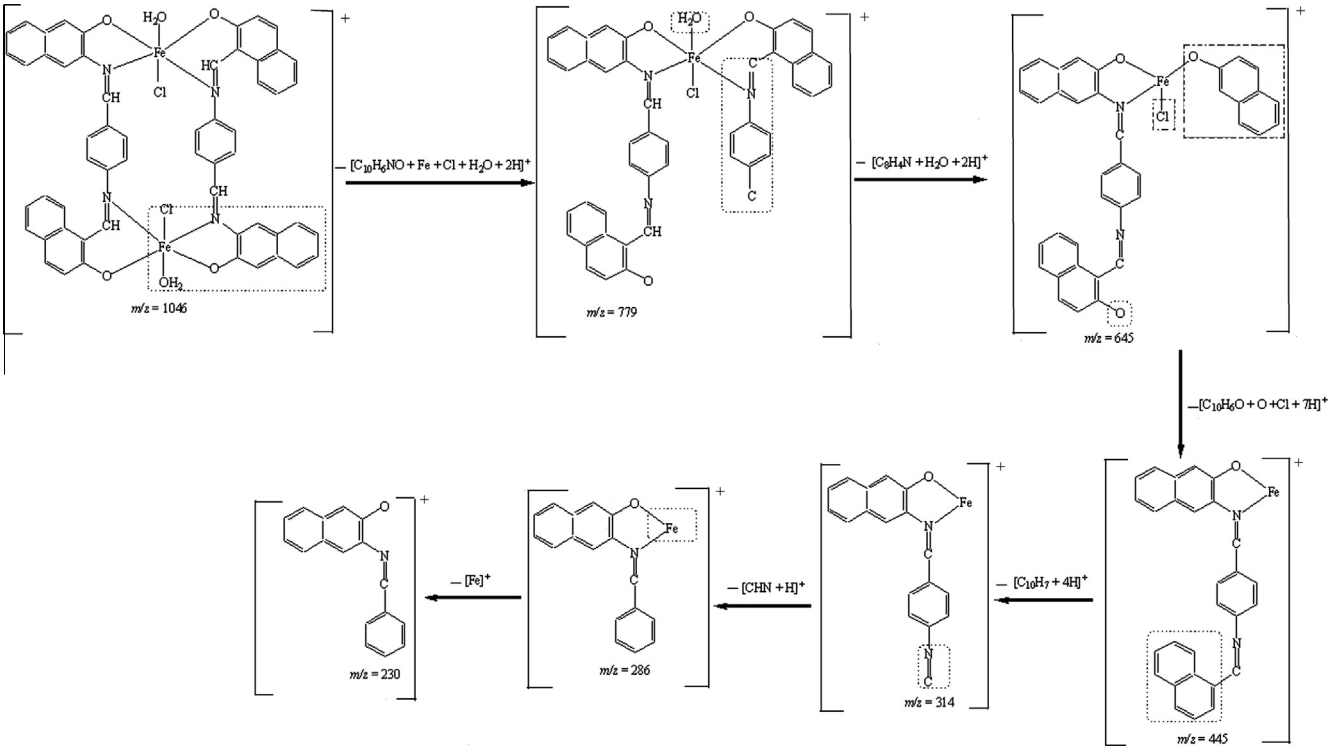

Figure 6 The fragments observed in mass spectra of $\mathbf{FeL^3}$.

be 0.63–41.96 Ω^{-1} cm^2 mol^{-1} in 10^{-3} M DMF or DMSO solutions. This fact indicates their nonelectrolytic nature (Geary, 1971).

3.3.1. Mass spectra

The mass spectra (ESI-positive) of the **NiL^1** and **FeL^3** (see Fig. 6) show the characteristic molecular ion $[M]^+$ peaks at the desired position for the dimeric structure, while **NiL^3**, **FeL^2** and **FeL^1** give the $[M+1]^+$, $[M+4]^+$ and $[M+6]^+$ peaks, respectively. The molecular ion peak of **NiL^2** could not be determined in the spectrum. The biggest fragment ion at m/z = 583.2 for **NiL^2** complex (see Fig. 7), loss of 261 mass unit from the dimeric $[Ni(C_{24}H_{16}N_2O_2)]_2$ unit, may suggest the expulsion of $[C_{18}H_{12}NO + 3H]^+$ unit from the dimeric molecule. In the spectra of **NiL^1**, **NiL^2** and **NiL^3**, the highest intensity peaks occurred m/z = 214 (100%), m/z = 264 (100%) and m/z = 314 (100%). The peaks at m/z = 214, m/z = 264 and m/z = 314 may correspond to $[C_{13}H_{14}N_2O]^+$, $[C_{18}H_4N_2O]^+$

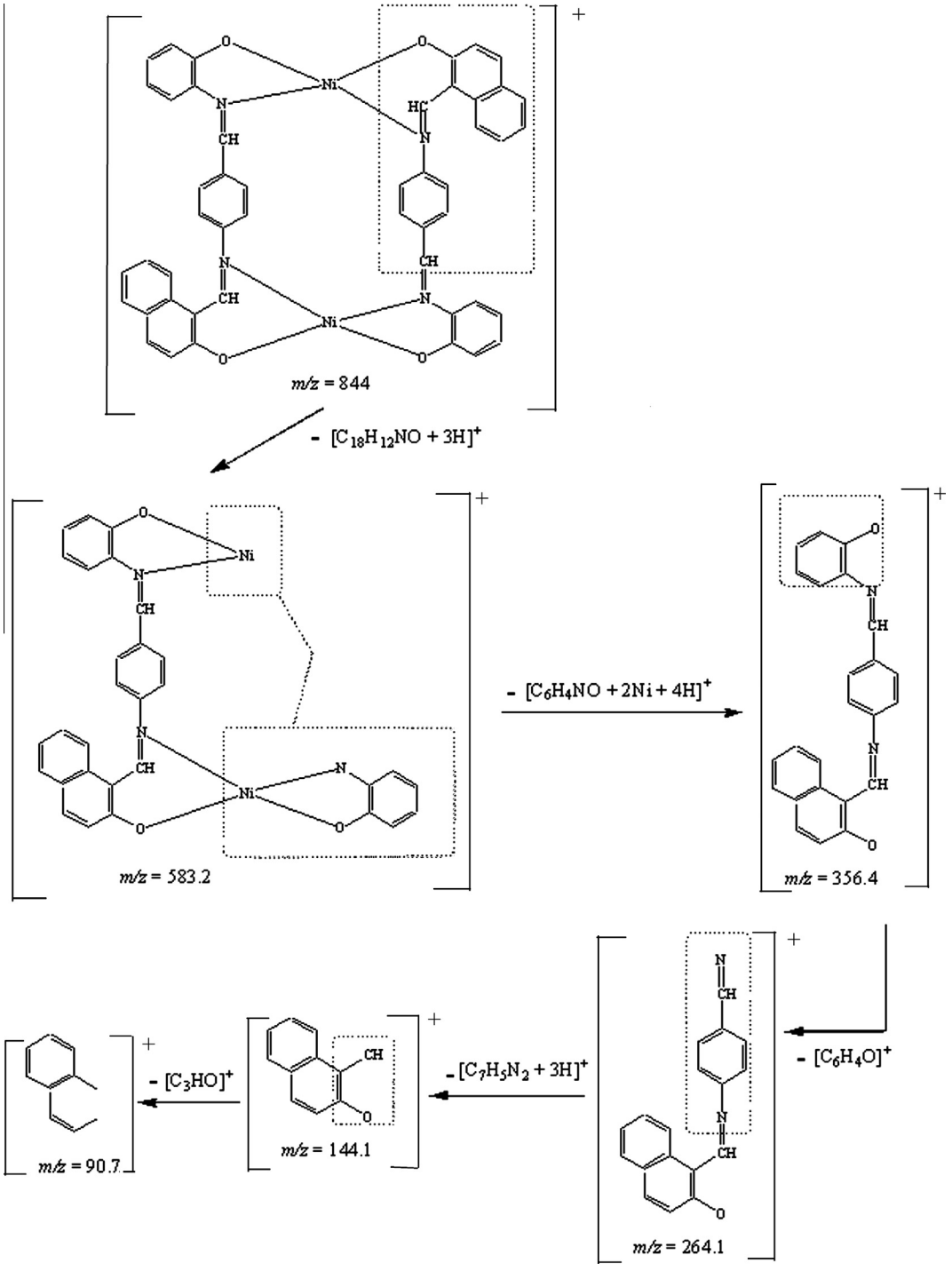

Figure 7 The fragments observed in mass spectra of **NiL^2**.

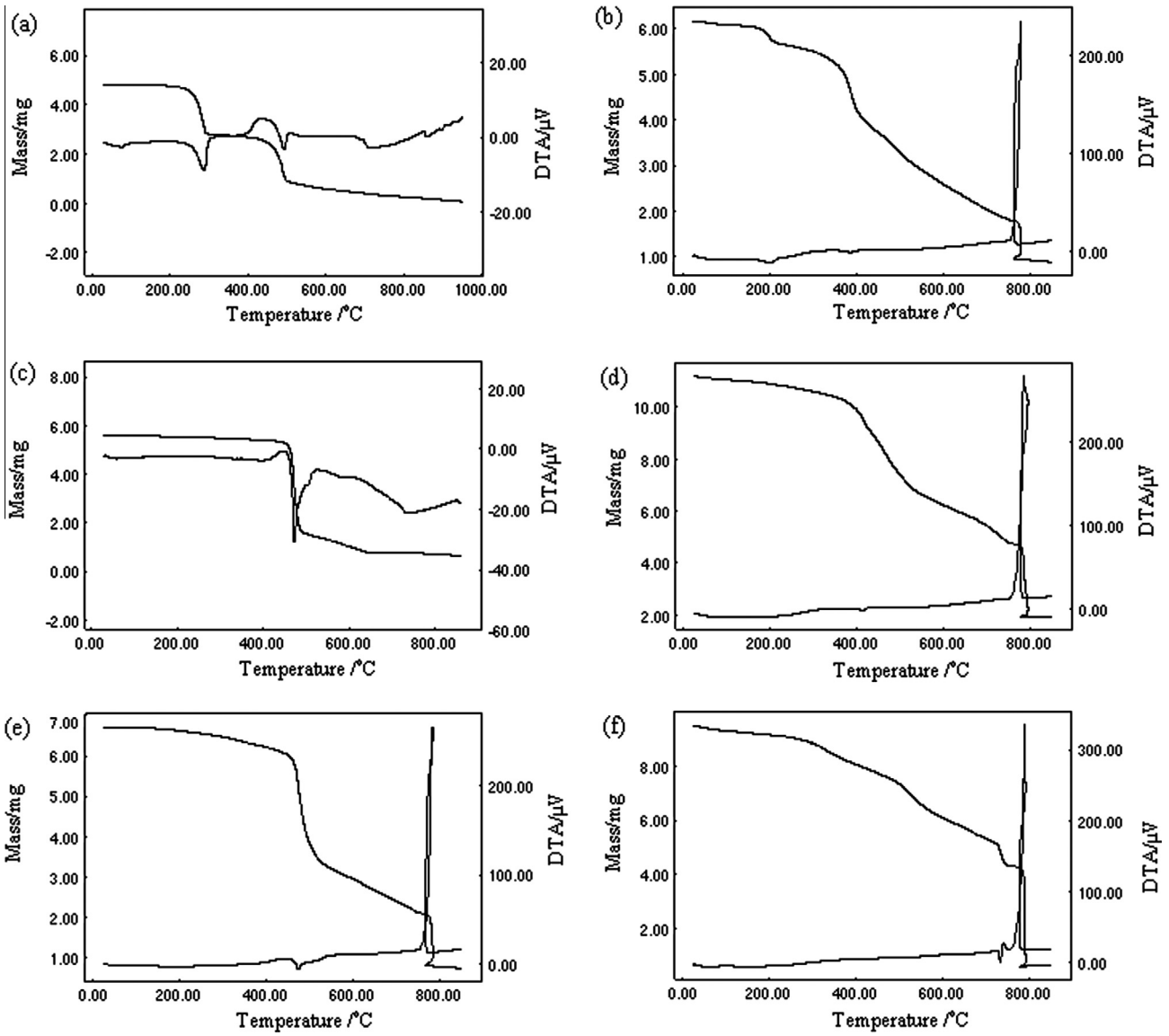

Figure 8 The TGA curves for (a) **NiL^1**; (b) **FeL^1**; (c) **NiL^2**; (d) **FeL^2**; (e) **NiL^3**; (f) **FeL^3**.

Table 2 Thermal data of the complexes.

Complex	1. Thermal reaction decomposition of H_2O molecules		2. Thermal reaction decomposition of the complex	
	Temperature range (°C)	% Mass loss found (Calcd.)	Temperature range (°C)	% Residue (NiO/Fe_2O_3) found (Calcd.)
NiL^1	83–260	8.80 (8.82)	432–800	17.30 (18.31)
FeL^1	45–205	6.20 (6.25)	320–711	16.80 (18.48)
NiL^2	–	–	430–800	16.40 (17.70)
FeL^2	51–266	3.80 (3.81)	Indefinite initiation and termination temperatures	17.20 (16.88)
NiL^3	–	–	419–726	16.10 (15.83)
FeL^3	52–242	3.40 (3.44)	Indefinite initiation and termination temperatures	12.90 (15.27)

Please cite this article in press as: Güngör, Ö., Gürkan, P. Potentiometric and antimicrobial studies on the asymmetric Schiff bases and their binuclear Ni(II) and Fe(III) complexes; synthesis and characterization of the complexes. Arabian Journal of Chemistry (2015), http://dx.doi.org/10.1016/j.arabjc.2015.02.009

Table 3 Powder X-ray diffraction data of complexes **NiL^2** and **FeL^2**.

Complex	Peak	2θ	d (Å)	Complex	Peak	2θ	d (Å)
$NiCl_2{\cdot}6H_2O$	1	5.0	17.66	**NiL^2**	1	4.5	19.62
	2	5.8	15.23		2	5.6	15.77
	3	7.2	12.27		3	7.2	12.27
	4	8.7	10.16		4	9.1	9.71
	5	16.3	5.43		5	11.7	7.56
	6	18.4	4.82		6	16.4	5.40
	7	20.5	4.33		7	18.7	4.74
	8	25.0	3.56		8	24.8	3.59
	9	29.8	3.00		9	25.8	3.45
	10	30.4	2.94		10	28.0	3.18
	11	31.2	2.86		11	30.4	2.94
	12	32.3	2.77		12	32.1	2.79
	13	33.2	2.70		13	37.0	2.43
	14	34.1	2.63		14	37.6	2.39
	15	35.3	2.54		15	42.1	2.15
	16	37.2	2.42		16	44.8	2.02
	17	39.6	2.27		17	46.0	1.97
	18	42.0	2.15		18	46.4	1.96
	19	43.0	2.10				
	20	44.0	2.06				
	21	45.0	2.01				
	22	46.5	1.95				
	23	47.5	1.91				
	24	49.1	1.85				
	25	49.8	1.83				
	26	51.6	1.77				
	27	53.5	1.71				
	1	4.3	20.50		1	3.1	28.48
	2	5.1	17.31		2	5.0	17.66
	3	7.8	11.33		3	5.2	16.98
	4	8.8	10.04		4	9.3	9.50
	5	9.1	9.71		5	11.1	7.97
	6	10.0	8.84		6	12.8	6.91
	7	13.9	6.37		7	13.0	6.80
$FeCl_3{\cdot}6H_2O$	8	14.8	5.98	**FeL^2**	8	16.2	5.47
	9	15.7	5.64		9	18.7	4.74
	10	17.6	5.04		10	19.2	4.62
	11	19.4	4.57		11	21.1	4.21
	12	22.0	4.04		12	22.1	4.02
	13	24.2	3.68		13	23.2	3.83
	14	25.8	3.45		14	26.0	3.42
	15	26.7	3.34		15	27.4	3.25
	16	28.3	3.15		16	28.3	3.15
	17	30.0	2.98		17	29.2	3.06
	18	32.4	2.76		18	30.3	2.95
	19	35.0	2.56		19	33.1	2.70
	20	37.2	2.42		20	35.3	2.54
	21	39.2	2.30		21	37.2	2.42
	22	41.7	2.16		22	39.2	2.30
	23	46.5	1.95		23	41.2	2.19
	24	51.8	1.76		24	42.0	2.15
	25	53.8	1.70		25	44.3	2.04
	26	59.1	1.56		26	54.2	1.69
					27	56.7	1.62
					28	59.6	1.55

Please cite this article in press as: Güngör, Ö., Gürkan, P. Potentiometric and antimicrobial studies on the asymmetric Schiff bases and their binuclear Ni(II) and Fe(III) complexes; synthesis and characterization of the complexes. Arabian Journal of Chemistry (2015), http://dx.doi.org/10.1016/j.arabjc.2015.02.009

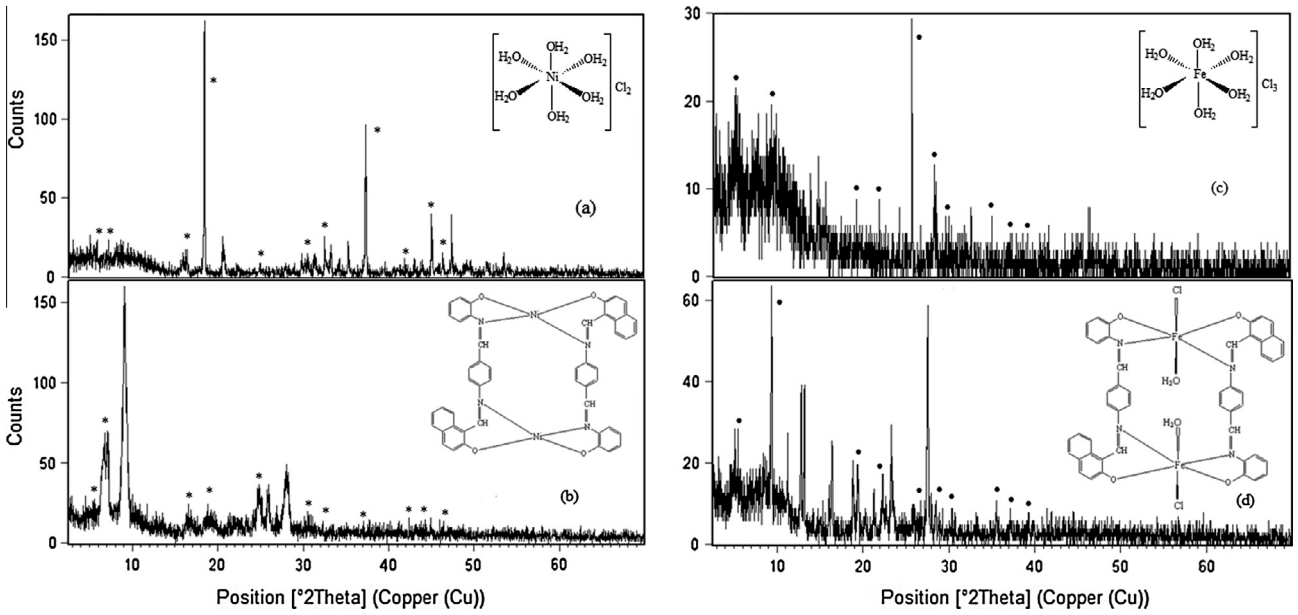

Figure 9 Powder XRD pattern of complexes (a) $NiCl_2{\cdot}6H_2O$; (b) **NiL²**; (c) $FeCl_3{\cdot}6H_2O$; (d) **FeL²**.

Table 4 Antimicrobial activities of the asymmetric diimines and their Ni(II) and Fe(III) complexes.

Compounds	Diameter inhibition zone (mm)			
	M. luteus (NRLL B-4375)	*B. cereus* (RSKK 863)	*E. coli* (ATCC 11230)	*C. albicans* (ATCC 10239)
H_2L^1 (500 μg)	38 (⩾32)[a]	10 (⩾125)	25 (⩾250)	24 (⩾63)
NiL^1 (67 μg)	36	4	15	16
FeL^1 (67 μg)	30	7	13	9
H_2L^2 (500 μg)	34	8	25	22
NiL^2 (67 μg)	33	0	9	10
FeL^2 (67 μg)	13	6	13	10
H_2L^3 (500 μg)	5	6	22	18
NiL^3 (67 μg)	22	0	0	6
FeL^3 (67 μg)	4	0	10	2
Erythromycin[b] (15 μg)	32	23	R[d]	–
Vancomycin[b] (30 μg)	28	12	R[d]	–
Oxiconazole[c] (0.2 μg/mL)	–	–	–	17
Isoconazole[c] (0.2 μg/mL)	–	–	–	17

[a] MIC values as ($\mu g\,mL^{-1}$).
[b,c] These values are taken from references (Nartop et al., 2008; Çete et al., 2006).
[d] Resistant.

and $[C_{21}H_{18}N_2O]^+$, respectively. In the spectra of **FeL^1**, **FeL^2** and **FeL^3**, the highest intensity peaks occurred m/z = 267 (100%), m/z = 395 (100%) and m/z = 445 (100%). The peaks at m/z = 267, m/z = 395 and m/z = 445 may correspond to $[C_{18}H_7N_2O]^+$, $[C_{24}H_7N_2OFe]^+$ and $[C_{28}H_9N_2OFe]^+$, respectively.

3.3.2. IR spectra

The two sharp bands between 1529–1573 cm^{-1} and 1598–1607 cm^{-1} for the Ni(II) complexes are assigned to both of the $\nu_{C=N}$ stretching vibrations. In the Fe(III) complexes, they appear at 1542–1574 cm^{-1} and 1579–1606 cm^{-1}. All of the $\nu_{C=N}$ bands are shifted to lower frequencies ca 6–30 cm^{-1} as compared to the free ligands (Güngör and Gürkan, 2010). This shows that the azomethine nitrogen atoms of the diimines are coordinated to metal ions which are further supported by the appearance of metal–nitrogen (M—N) bands at between 434 and 476 cm^{-1}. In the IR spectra of the complexes, except for **NiL^2**, phenolic ν_{OH} bands disappeared on complexation compared with that of the free ligands (Güngör and Gürkan, 2010). This fact suggests that the phenolic oxygen atoms of the diimines participate in the coordination to the metal ions. All the complexes show ν_{M-O} (phenolic) bands at 457–573 cm^{-1}. The medium broad bands appear at 3300–3436 cm^{-1} for Fe(III) complexes and **NiL^1** are assigned to the ν_{OH} vibrations of coordinated water.

Please cite this article in press as: Güngör, Ö., Gürkan, P. Potentiometric and antimicrobial studies on the asymmetric Schiff bases and their binuclear Ni(II) and Fe(III) complexes; synthesis and characterization of the complexes. Arabian Journal of Chemistry (2015), http://dx.doi.org/10.1016/j.arabjc.2015.02.009

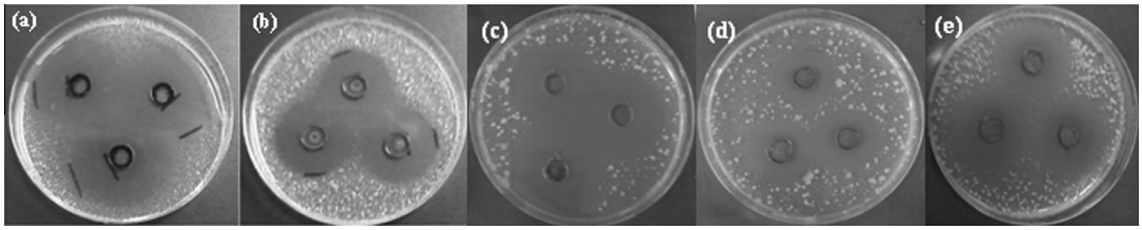

Figure 10 The diameter inhibition zones for (a) **FeL^1** and (b) **NiL^3** against *M. Luteus*; (c) **H$_2$L^1** and (d) **H$_2$L^3** against *C. albicans*; (e) **H$_2$L^2** against *E. coli*.

3.3.3. Magnetic susceptibilities and electronic spectra

NiL^2 and **NiL^3** complexes are diamagnetic, suggesting the square planar geometry. **NiL^1** complex has a magnetic moment of 2.59 BM; 1.30 BM per Ni(II) ion. This value is considerably less than the expected values for two spin-free Ni(II) ions present in the same molecular unit, indicating strong metal–metal interaction in the dimeric structure (Lal et al., 2009; Nag et al., 2005).

Electronic spectra of the paramagnetic **NiL^1** complex, the new bands at 421 nm and 750 nm assign to $^3A_{2g} \rightarrow {}^3T_{2g}$ and $^3A_{2g} \rightarrow {}^3T_{1g}$ transitions for octahedral d^8 ions. In the electronic spectra of square-planar **NiL^2** and **NiL^3** complexes, a weak absorption bands at 448 nm and 442 nm indicate $^1A_{1g} \rightarrow {}^1A_{2g}$ transition for d^8 ions.

All the dimeric Fe(III) complexes show slightly lower μ_{eff} values than the spin-only values for the high spin octahedral Fe(III) complexes. These values are indicative of interaction between two Fe(III) centers in the dimeric molecules (Dubey et al., 2006).

3.3.4. Thermal studies

The TGA curves of the complexes are given in (Fig. 8(a–e)). Full thermoanalytical data of the complexes are given in Table 2. In TGA curves, **NiL^1** decomposes in two steps. Mass loss in the first thermal reaction is observed at temperatures between 83 and 260 °C, corresponding to the four moles of coordinated water molecule in the complex. **NiL^2** and **NiL^3** decomposed in one step. The endothermic peaks lying at ca 430–536 °C for all of the Ni(II) complexes correspond to melting. The residues at the end of the decomposition for all of the complexes are found to be NiO and the percent of metal ion is calculated.

In TGA curves, all of the Fe(III) complexes decompose in two steps. The initial mass loss occurs at ca 45–266 °C range for complexes; this mass loss seems to be consistent with evaluation of the one mole hydration water molecule and/or two coordination water molecules in the complex. The endothermic peaks lying at ca 364–410 °C for **FeL^1** and 380–443 °C for **FeL^2** were due to melting. The residues at the end of the decomposition for all of the complexes are found to be Fe_2O_3 and the percent of metal ion is calculated.

3.3.5. Powder X-ray diffraction studies

The powder XRD patterns of all the complexes were recorded at $2\theta = 0$–$70°$ range. The X-ray diffractograms, the '*d*' values and 2θ angles of **NiL^2** and **FeL^2** complexes are given in Fig. 9 and listed in Table 3. The spacing between the planes in the atomic lattice (*d*) was calculated using Bragg's formula as follows:

$$n \cdot \lambda = 2 \cdot d \cdot \sin\theta$$

where '*n*' is an integer ($n = 1$), 'λ' is the wavelength ($\lambda = 1.54059$ Å) and 'θ' is the peak angle.

The diffractogram of **NiL^2** complex has recorded 18 reflections of 2θ ranging from 4.5° to 46.4°. The maximum recorded is at 9.1°. The observed $\sin\theta$ value and *d* values obtained have been compared with $NiCl_2{\cdot}6H_2O$. The diffractogram of **FeL^2** complex showed 28 reflections between 2θ ranging from 3.1 to 59.6 with maxima peaks at $2\theta = 9.3°$ and 27.4°. The observed sinθ value and *d* values obtained have been compared with $FeCl_3{\cdot}6H_2O$.

All of the Ni(II) and Fe(III) complexes show well defined sharp peaks. This shows that the above complexes are crystalline in nature (Nair and Joseyphus, 2008). The line broadening of the crystalline diffraction peak in the Ni(II) complexes shows higher crystallinity than that of Fe(III) complexes by comparing the diffractograms.

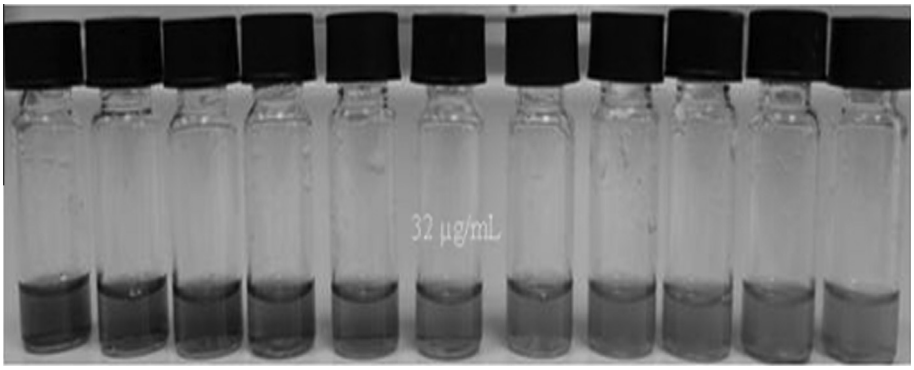

Figure 11 The minimum inhibitory concentration (MIC) value of **H$_2$L^1** against *M. Luteus* (left to right: 1000, 500, 250, 125, 63, 32, 16, 8, 4, 2, 1 µg/mL).

Please cite this article in press as: Güngör, Ö., Gürkan, P. Potentiometric and antimicrobial studies on the asymmetric Schiff bases and their binuclear Ni(II) and Fe(III) complexes; synthesis and characterization of the complexes. Arabian Journal of Chemistry (2015), http://dx.doi.org/10.1016/j.arabjc.2015.02.009

3.4. Antimicrobial activities

The antimicrobial activity of the asymmetric diimines and their Ni(II) and Fe(III) complexes were tested against bacteria: *M. luteus* (NRLL B-4375), *B. cereus* (RSKK 863), *E. coli* (ATCC 11230) and the fungus: *C. albicans* (ATCC 10239). The diffusion agar technique was used to determine the antimicrobial activity (Çete et al., 2006). The results of antimicrobial screening of the compounds are summarized in Table 4.

As can be seen in Table 4, $\mathbf{H_2L^1}$ diimine and its Ni(II) and Fe(III) complexes have an antimicrobial activity on all the studied microorganisms. Because of the biggest activity of $\mathbf{H_2L^1}$ against all the studied microorganisms, its minimum inhibitory concentration (MIC; μg mL^{-1}) was determined. It shows high levels of antimicrobial activity against *M. luteus* (Figs. 10(a) and 11) and *C. albicans*. $\mathbf{H_2L^2}$ diimine and its Fe(III) complex show antimicrobial effect on the microorganisms, whereas $\mathbf{NiL^2}$ complex is inactive against *B. cereus*. While $\mathbf{H_2L^3}$ diimine exhibits activity against the microorganisms, $\mathbf{NiL^3}$ complex is inactive against *B. cereus* and *E. coli*; $\mathbf{FeL^3}$ complex does not show any effect against *B. cereus*. Table 4 shows that *E. coli* is the most influenced bacteria against all of the diimines and the diameter inhibition zones (34 mm) of $\mathbf{H_2L^2}$ diimine are the biggest against *M. luteus*. Moreover, all of the diimines have an activity on *C. albicans*. In all bacteria, *M. luteus* is the most influenced bacteria against Ni complexes, in the 36–22 mm diameter inhibition zones ranges. Between the Ni(II) complexes, $\mathbf{NiL^1}$ exhibits the most activity against the tested bacteria. For the Fe(III) complexes, $\mathbf{FeL^1}$ has the biggest diameter zones (30 mm) against *M. luteus* (Fig. 9(a)). The fungicidal screening shows that *C. albicans* is the most influenced against $\mathbf{NiL^1}$ complex, having the diameter zones of 16 mm and $\mathbf{FeL^3}$ complex shows quiet activity against this fungi.

Acknowledgments

The authors are grateful to Research Foundation of Gazi University for supporting this study with the Project F.E.F.05/2008-07. And the authors thank to Mr. Servet Çete for his studies on antimicrobial activities of the compounds.

References

Belaid, S., Djebbar, S., Benali-Baitich, Q., Khan, M., Bouet, G., 2007. C. R. Chimie 10, 568.
Çete, S., Dişli, A., Yıldırır, Y., Yaşar, A., 2006. Asian J. Chem. 18, 2061.
Dubey, R.K., Dubey, U.K., Mishra, C.M., 2006. Trans. Met. Chem. 31, 849.
Galic, N., Cimerman, Z., Tomisic, V., 1997. Anal. Chim. Acta 343, 135.
Geary, W.J., 1971. Coord. Chem. Rev. 7, 81.
Gran, G., 1952. Analyst 77, 661.
Gündüz, T., Kılıç, E., Canel, E., Köseoğlu, F., 1993. Anal. Chim. Acta 282, 489.
Güngör, Ö., Gürkan, P., 2010. Spectrochim. Acta A 77, 304.
Güngör, Ö., 2008. M.Sc. Thesis. Gazi University, Ankara.
Hernández-Molina, R., Mederos, A., Gili, P., Domínguez, S., Núñez, P., Germain, G., Debaerdemaeker, T., 1997. Inorg. Chim. Acta 256, 319.
Hou, Q., Zhao, L., Zhang, H., Wang, Y., Jiang, S., 2007. J. Lumin. 126, 447.
Hökelek, T., Kılıç, Z., Işıklan, M., Toy, M., 2000. J. Mol. Struct. 523, 61.
Irving, H., Rossotti, H.S., 1954. J. Chem. Soc., 2910
Kumari, N., Prajapati, R., Mishra, L., 2008. Polyhedron 27, 241.
Köseoğlu, F., Kılıç, E., Uysal, D., 1995. Talanta 42, 1875.
Lal, R.A., Choudhury, S., Ahmed, A., Chakraborty, M., Borthakur, R., Kumar, A., 2009. J. Coord. Chem. 62, 3864.
Martell, A.E., Motekaitis, R., 1988. Determination and Use of the Stability Constants. VCH Publisher, New York.
Mashhadizadeh, M.H., Sheikhshoaie, I., Saeid-Nia, S., 2003. Sens. Actuators B 94, 241.
Nair, M.S., Joseyphus, R.S., 2008. Spectrochim. Acta A 70, 749.
Nag, J.K., Pal, S., Sinha, C., 2005. Trans. Met. Chem. 30, 523.
Nartop, D., Gürkan, P., Sarı, N., Çete, S., 2008. J. Coord. Chem. 61, 3516.
Sarı, N., Gürkan, P., Arslan, S., 2003. Trans. Met. Chem. 28, 468.
Shokrollahi, A., Abbaspour, A., Ghaedi, M., Naghashian Haghighi, A., Kianfar, A.H., Ranjbar, M., 2011. Talanta 84, 34.
Sürücüoğlu, K., 2008. PhD. Thesis. Gazi University, Ankara.
Sözen, P., Akgül, Y., Demirhan, F., 2007. Turk. J. Chem. 31, 201.
Ünver, H., Kabak, M., Zengin, D.M., Durlu, T.N., 2001. J. Chem. Crystallogr. 31, 203.
Ünver, H., Yıldız, M., Kiraz, A., İskeleli, N.O., Erdönmez, A., Dülger, B., Durlu, T.N., 2006. J. Chem. Crystallogr. 36, 229.
Van Uitert, L.G., Haas, C.G., 1953. J. Am. Chem. Soc. 75, 451.

Please cite this article in press as: Güngör, Ö., Gürkan, P. Potentiometric and antimicrobial studies on the asymmetric Schiff bases and their binuclear Ni(II) and Fe(III) complexes; synthesis and characterization of the complexes. Arabian Journal of Chemistry (2015), http://dx.doi.org/10.1016/j.arabjc.2015.02.009